Journal of the Textile Institute
Publication details, including instructions for authors and subscription information:
http://www.informaworld.com/smpp/title~content=t778164490

Compression and permeability properties of multiaxial warp-knit preforms

Naveen V. Padaki[a]; R. Alagirusamy[a]; B. L. Deopura[a]; R. Fangueiro[b]
[a] Department of Textile Technology, Indian Institute of Technology-Delhi, New Delhi, India [b] Department of Textile Engineering, University of Minho, Guimarães, Portugal

To cite this Article Padaki, Naveen V. , Alagirusamy, R. , Deopura, B. L. and Fangueiro, R.(2008) 'Compression and permeability properties of multiaxial warp-knit preforms', Journal of the Textile Institute, 99: 4, 287 — 294
To link to this Article: DOI: 10.1080/00405000701414733
URL: http://dx.doi.org/10.1080/00405000701414733

Taylor & Francis
Taylor & Francis Group

Compression and permeability properties of multiaxial warp-knit preforms

Date Submitted 1 February 2007, Date Accepted 18 April 2007 doi:10.1080/00405000701414733

Naveen V. Padaki[1], R. Alagirusamy[1], B. L. Deopura[1] and R. Fangueiro[2]

[1]*Department of Textile Technology, Indian Institute of Technology-Delhi, Hauz Khas, New Delhi 110 016, India*
[2]*Department of Textile Engineering, University of Minho, 4800-058-Guimarães, Portugal*

Abstract: Textile preform properties such as compression and permeability greatly influence the quality of the composite material and its performance, particularly those prepared by injection moulding techniques like resin transfer moulding (RTM). Directionally oriented warp-knit biaxial, triaxial and quadraxial glass fabrics have been studied for these preform properties. The preform compression properties were tested on the universal testing machine up to a maximum force of 250 N. The rate of test liquid flow through these preforms has been measured using the horizontal wicking test method. The permeability of these preforms has been analyzed based on the liquid flow-rate data. Fibre orientation and fibre volume fraction of the preforms are observed to be important factors influencing these preform properties.

Key words: Textile preforms, multiaxial warp knits, compression, permeability.

INTRODUCTION

Textile-reinforced composites have been used successfully from many decades as engineering materials, designed and manufactured for various applications such as maritime craft, aircraft, automobile, civil and many structural end uses. Major advantages such as ease of handling, net-shapability and highly versatile design potential due to structural complexity (Chou, 1992) have made the textile preforms a prime reinforcement for composite applications. The three-dimensional textile preforms offer improved damage tolerance and the benefit of near-net-shape manufacturing (Kamiya *et al.*, 2000). Amongst these preforms, directionally oriented structures (DOS) or multiaxial warp knits (MAWK) have been evolved through structural modifications of warp-knitted fabrics with inlay yarns in desired directions. They are also termed as non-crimp structures since the presence of knitted loops is to perform the function of holding layers of uncrimped inlay yarns (Anand, 1996). Amount of fibre and orientation in controlled directions play a critical role in preform engineering, wherein the mechanical properties of the composite are mainly designed according to the fibre properties. Liba and Malimo systems along with such inlay knit layers can as well incorporate fibre or non-woven fleece between the layers to produce multiaxial multilayer structures (Padaki *et al.*, 2006), whole of these DOS are predominantly applied for composite reinforcements (Du and Ko, 1996).

An ever-increasing demand for faster composite manufacture has pressed the composite industry to replace hand lay-up technique with alternative liquid composite moulding (LCM) techniques such as RTM, in which the preform characteristics influence composite manufacture to a great extent. Current advances in research are focused on quality reinforcement production for the final component so as to achieve process times compatible with liquid injection methods. Preform characteristics are ascertained to influence the quality, properties and performance of composite materials prepared by the LCM processes. Type of the reinforcement, fibre orientation, compression behaviour and permeability characteristics are the major influencing factors in this aspect.

During the use of textile preforms in the process of liquid injection composite preparations, resin flow–induced defects, voids and dry (resin-less) spots are considered to be the largest source of quality and reproducibility problems (NIST, 1990). These defects are mainly due to unbalanced resin flows, which are directly related to variations in the permeability of the fibre preform. Poor fibre preform

Corresponding author:
N. V. Padaki
Department of Textile Technology
Indian Institute of Technology—Delhi
Hauz Khas, New Delhi 110 016
India
Tel: 0091-11-26591419; Fax: 0091-11-26581103
Email: naveenvpadaki@gmail.com

quality, fabric deformation, or improper fibre preform preparation/loading are reported to be leading causes for variations in permeability (Lai and Young, 1997; Sridhar *et al.*, 1998). In conventional experimental studies, fibre permeability is typically measured using specially designed transparent molds. Although preforms are in reality easily deformed and re-structured during the composite manufacturing, understanding of permeability properties of such preforms definitely help in better and faster composite preparation.

Fluid permeability through a fibrous preform is by a combinational process of wetting and wicking (Patnaik *et al.*, 2006). Wetting is the initial process involving the fluid spreading wherein the fibre–air interface is displaced with the fibre–liquid interface. Wetting is measured in terms of the contact angle, which is formed by the substrate and the tangent to the surface of the liquid droplet at the contact point. Contact angle measurement is a precise empirical tool to determine the wetting interaction between a liquid (surface tension) and a substrate (surface free energy). Wicking is the capillary flow of liquid through the porous preform due to the difference in fluid pressure. Fluid pressure and flow rate measurements from the above are used to obtain an average permeability for the preform using Darcy's law for a linear and slow steady-state flow as given by Darcy's equation (1)

$$Q = -K\frac{\Delta P}{L} \quad (1)$$

where K is the permeability constant of the porous medium, ΔP the net flow pressure head and L the length of the sample in the direction of flow. The permeability constant (K) is a characteristic value of the fabric which does not change with different fluids; it is expressed as a ratio of the permeability (k) of the media to the fluid viscosity (η), as given by equation (2). A few studies have indicated that the effect of fluid in such preform permeability studies has less significance (Han *et al.*, 2000; Luo *et al.*, 2001). From the above relations, it is clear that as the fluid viscosity changes, permeability (k) changes accordingly.

$$K = \frac{k}{\eta} \quad (2)$$

Another important property of the textile preforms for composite reinforcement is the compressibility, which influences the preform porosity, as many of the textile structures are readily deformable due to mould closing and pressure or vacuum application during composite manufacture by injection moulding methods. Compressibility of textile reinforcements not only influences the fibre architecture but also affects the permeability through porosity variations and hence the composite manufacturing process (Pillai *et al.*, 2001). When the fibrous preform is subjected to compression it undergoes a number of changes, such as flattening of fibrous tow, reduction of the pores and gaps between the fibres inside tows as well as between individual tows, elastic deformation, inter-layer shifting (nesting), etc.

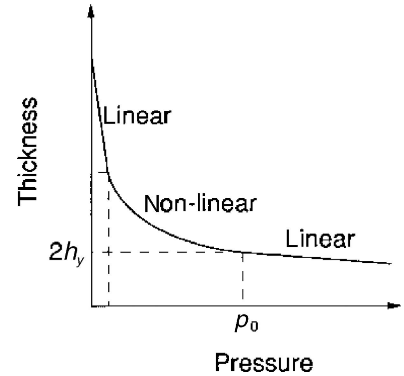

Figure 1 Typical compression behaviour of textile preforms [13].

A typical compression pressure versus preform thickness curve for a woven fabric is depicted in Figure 1 (Chen and Chou, 1999). Initial preform compaction is primarily due to the reduction of pores and gaps among the fibres and yarns, while at higher pressure, compression is dominated by the bending deformation of yarns. The woven fabric compressibility model was first proposed by van Wyk (1946) considering the fibres as beams in Kirchhof bending. Furthermore, Gutowski *et al.* (Cai and Gutowski, 1992; Gutowski, 1985; Gutowski and Dillon, 1992, 1997) have made contributions to the theoretical modelling of fabric compressibility based on this beam theory. Various fabric compressibility models have been reviewed (Hu and Newton, 1997) and many studies have attempted to relate compaction pressure with preform thickness by regression analyses (Matsudaira and Qin, 1995; Pearce and Summerscales, 1995; Saunders *et al.*, 1998, 1999; Toll and Manson, 1994). Hoffman and Beste (1951) had initially proposed an exponential thickness–pressure function for fabrics. Preform compression behaviour has been reported in detail using five parameters: initial fibre volume fraction, final fibre volume fraction, initial preform bulk compressibility, fibre solid compressibility and an empirical exponent for power-law (Chen *et al.*, 2001). The present study is an attempt to understand these compressive and permeability behaviour of directionally oriented warp-knit preforms for composite reinforcement applications. The variation of preform thickness due to compressive force, experimental fluid flow behaviour and permeability properties of biaxial, triaxial and quadraxial warp-knit glass preforms are studied and the rationalization of influence of preform compression on the permeability has been tried.

MATERIAL AND METHODS

Materials

Multiaxial warp-knit preforms as represented by line diagrams in Figure 2 (Raz, 2000), i.e., biaxial, triaxial and quadraxial structures were used for the present studies. The E glass fibres were used as inlay and polyester (50 denier) was used as the knitting yarn. Fabric characteristics

Table 1 **Multiaxial warp-knit fabric specifications**

Preform	Glass inlay yarn, Tex (inlay direction)	Preform thickness (at 5 N), mm (CV%)	Weight, g/m^2 (CV%)
Biaxial DOS	200 (+45,–45)	0.81 (2.8)	406 (4.3)
Triaxial DOS	900 (0) 300 (+45,–45)	1.12 (3.4)	787 (3.5)
Quadraxial DOS	600 (0) 300 (+45,–45,90)	1.62 (2.1)	802 (2.9)

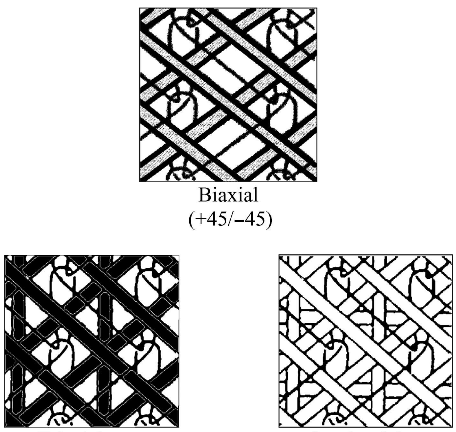

Figure 2 Directionally oriented warp-knit structures.

and construction details are presented in Table 1. The inlay E glass roving in different directions are mentioned as 0° along wale, 90° along course and ±45° along bias directions.

Preform testing

Compression test

The compression behaviour of these preforms was tested on Hounsfield H100KS universal testing machine (compression head area 25.16 cm^2) at a rate of 5 mm/min. Preform compression behaviour as a function of applied force to a maximum of 250 N was carried out with an initial preload of 5 N; for each preform 30 tests were done. The data obtained as fabric compression (mm) to the applied force (N) were stored to plot and calculate the results.

Permeability—Horizontal wicking test and contact angle wettability tests

The tests conducted for the permeability studies include horizontal or in-plane wicking test and contact angle wettability tests. The preforms were preconditioned per ASTM standard D1776 and 10 trials in each test were done for each of the above-mentioned samples.

Water wicking of the said preforms was obtained by measuring the wicking rate (g/min) using a horizontal in-plane wicking tester (Fig. 3) developed in the department of textile technology, Indian Institute of Technology—Delhi, India. In this instrument, a tiny water front is presented to the horizontally placed fabric sample (size 16 cm × 16 cm), which starts to absorb the water by wicking due to capillary action through the pores within the yarn and fabric structure. The water is supplied continuously from a reservoir by siphoning. The reservoir is kept on a digital weighing balance, which enables recording of data for the mass of water absorbed by the fabric.

Another wicking experiment to saturation was carried on 10 cm × 10 cm sample of the preform in which average time for sample saturation is obtained. This type of flow measurement could be of immense use to compare different preforms for flow patterns and the data obtained from this study was used to calculate the permeability. In the first set of trials in this experiment, the amount of water required for saturation was noted for five specimens. A second set of trials with another five specimens was carried out to estimate the time required for that average amount of water to be wicked. By this, permeability in terms of water wicked per unit time per unit area could be arrived at to compare the fluid flow rate through the different preforms conveniently. Wettability tests on the preforms were carried out using automated Contact Angle tester per the standard D5725 (ASTM International, 2003).

RESULTS AND DISCUSSIONS

Figure 4 illustrates the compression behaviour of the textile preforms under investigation. The preforms are compressible to one-third of their thickness and the behaviour can be segregated into three types: initial linear trend, mid-nonlinear, followed by final linear behaviour. Initially under the action of compression forces on preform, the pore volume reduces rapidly to bring the fibres close to each other. This initial phase could be recognized from the figure as the first linear segment, which requires less force for compression. In the second, curvilinear stage, the fibres realign themselves and are rearranged involving fibre bending. Hence this phase requires more force compared to the first and the higher compression resistance could be due to the bending modulus of the fibres in preform. The final stage, which involves compressing the fibres themselves, is represented by last linear segment of the diagram.

Exponential curve-fitting technique was adopted to establish an empirical relation between the compressive force P with a corresponding change in preform thickness t as given by equation (3), where C and α are constants. The change in preform thickness t is the difference of initial

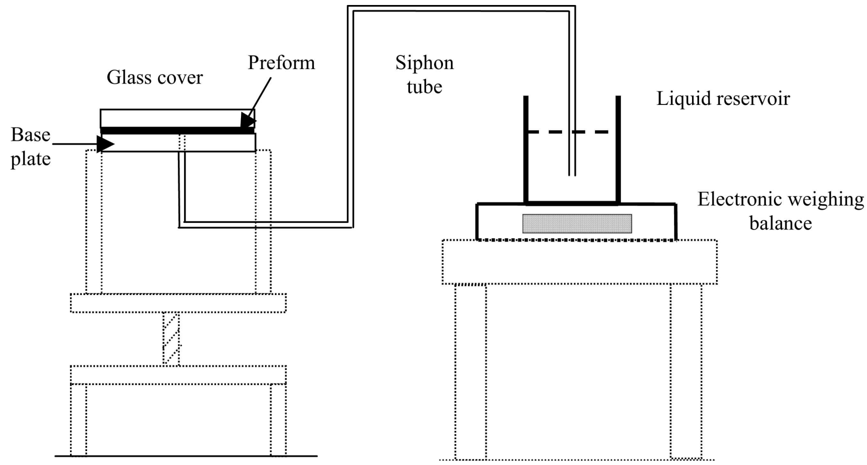

Figure 3 Horizontal wicking tester.

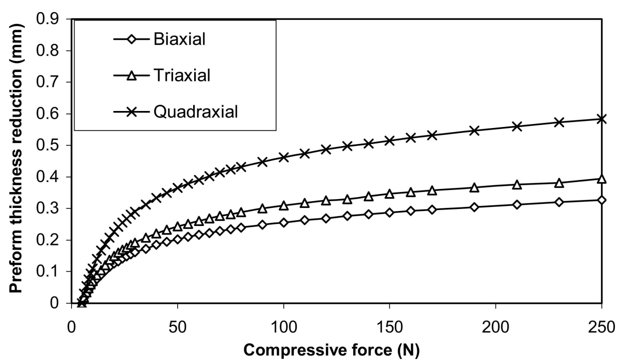

Figure 4 Compression behaviour of preforms.

preform thickness (t_i) from that at compressive force P (t_P), expressed by equation (5). The relation (3) can be expressed in terms of change in preform thickness t, as given by equation (4). A mathematical equation as represented below by equation (6) from equations (4) and (5) to estimate the behaviour of these preforms under compression, where ΔV_f is the change in fibre volume fraction resulting from reduction in the fabric thickness and applied compressive force, assuming negligible change in aerial density of the fabric. The values of constants C and α of the equation for each type of preform are tabulated (Table 2) after analyzing the test data. Fibre volume fraction in the preform is the ratio of volume occupied by the fibre to that of the fabric, calculated from fabric aerial weight, fibre density (glass 2.5 g/mm^3) and preform thickness. It could be noticed from the Table 2 that with increase in the fibre volume fraction of the preform, the resistance to compression also increases. Biaxial and quadraxial warp-knit preforms have the least fibre volume fraction and they show the highest preform compressibility.

$$P = C.e^{\alpha . t} \tag{3}$$

$$t = \frac{\ln(P) - \ln(C)}{\alpha} \tag{4}$$

$$t = t_i - t_P \tag{5}$$

$$\Delta V_f = \frac{t_i - t_P}{t_i} = \frac{\ln(P) - \ln(C)}{t_i \alpha} \tag{6}$$

Table 3 presents the results of horizontal wicking test with respect to the flow rate, amount of water wicked by the preforms after the first minute and 5 minutes of testing. Figure 5 illustrates the permeability of preform in terms of fluid flow rate from the horizontal wicking test. It can be observed that among the DOS, quadraxial preforms have the highest amount of water wickability, followed by triaxial structures and the least for the biaxial preforms. The results imply that fibre orientation in the preform plays a significant role in wicking, with higher isotropicity of the fibres effecting greater wickability.

Wettability tests on the directionally oriented warp-knit preforms by automated contact angle tester reveal that the spreading time of water droplets on these preforms is very less to the tune of milliseconds. This behaviour could be due to the high surface energy of glass, surface finishes applied on the glass fibres to make them easily wettable and

Table 2 **Compression test data of preforms**

Preform	Fibre volume fraction (5 N)	Fibre volume fraction (250 N)	Reduction in preform thickness (250 N), mm (CV%)	C	A	R^2
Biaxial DOS	0.20	0.31	0.28 (2.3)	4.62	12.0	0.99
Triaxial DOS	0.28	0.35	0.23 (1.9)	4.75	9.89	0.98
Quadraxial DOS	0.20	0.29	0.58 (1.7)	4.57	6.70	0.99

Table 3 **Wicking and permeability properties of preforms**

Preforms	Fibre diameter, μm	Amount of water wicked (1 min), g (CV%)	Amount of water wicked (5 min), g (CV%)	Flow rate, 10^{-2} g/(cm^3 s) (CV%)	Hydraulic radius of fibre bed (m), μm	Flow length (L), cm at 60 s	Pressure difference (ΔP), 10^3 dyne/cm^2	Permeability constant (K), 10^{-7} s	Permeability (k), 10^{-9} g/cm^2
Biaxial DOS	12	2.96 (4.2)	9.44 (3.3)	3.77 (4.1)	12	3.12	60.0	1.96	1.74
Triaxial DOS	14	5.93 (4.7)	16.54 (3.9)	4.19 (3.7)	9	2.70	80.0	1.41	1.26
Quadraxial DOS	14	12.86 (3.9)	33.44 (2.6)	6.50 (3.7)	14	3.37	51.43	4.25	3.79

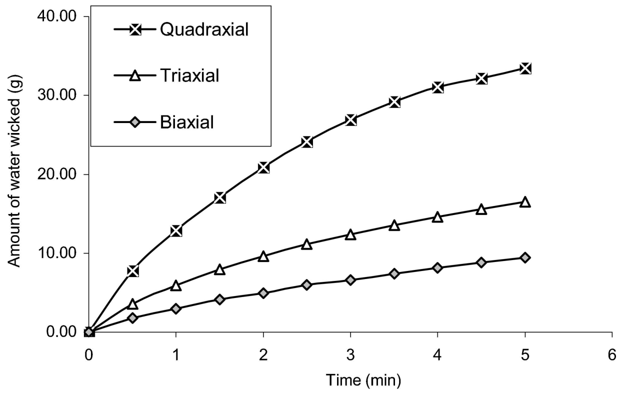

Figure 5 Wickability of preforms (amount of water wicked by the preform vs time).

low fibre diameter of the glass fibres. Hence for calculation purposes, *cos* θ was presumed as 1, since θ is close to 0°.

The flow rate tests on 10 cm × 10 cm samples near saturation point to some interesting observations. Instantaneous initial wicking along the fibre orientation directions, then flow reaching in other directions taking more time followed by overflow from the boundaries of the preform, has been noticed repeatedly. Instantaneous wicking can be attributed to the presence of lucid fibre capillaries along the fibre orientation direction and the slow fluid flow in other directions could be due to the discontinuous capillaries between fibre–fibre and fibre–plate regions. Although flow front reaches the preform boundary, overflow commences much later than the earlier-mentioned flows. This overflow could be due to the higher fluid pressure between the top and the bottom plate than the surface tension in the fluid–plate region, which would result from a saturation of the preform and continuous water feed.

From Darcy's law of fluid flow through a porous media, ΔP—the difference in fluid pressure—is the sum of the external fluid flow pressure difference and the internal capillary pressure ($P + P_c$). This capillary pressure, P_c (dyne/cm^2), is given by equation (7) (Luo *et al.*, 2001)

$$P_c = \frac{\gamma \cos\theta}{m} \tag{7}$$

where γ is the surface tension of the fluid (72 dyne/cm^2 for water), θ is the wetting angle (contact angle) and m is the hydraulic radius of the fibre bed (cm). This hydraulic radius of the fibre bed, m, is expressed in terms of capillary radius (R_c) as the ratio of capillary cross-sectional area normal to the flow and its wetted perimeter, given by equation (8) as follows,

$$m = \frac{\Pi R_c^2}{2\Pi R_c} = \frac{R_c}{2} \tag{8}$$

The fibre bed hydraulic radius m is calculated by equation (9) (Luo *et al.*, 2001) as

$$m = F.\frac{d_f}{4}.\frac{1 - V_f}{V_f} \tag{9}$$

where d_f, the fibre diameter (cm), V_f, the fibre volume fraction and F is a function of fabric geometry (tortuosity, $F = 1$ for UD fibre beds). For the multiaxial warp-knit DOS structures, F was assumed to be 1 as the inlay layers consist of glass filaments in specified directions without any interlocking or interlacement; therefore, the capillaries are similar to those of UD fibre beds. The fibre diameter was measured optically by microscopic observation of cross section of composite made from these preforms. Higher wettability (contact angle nearing 0°) and smaller capillary radius induce higher capillary pressure, as elucidated by equation (7). Preform volume fraction becomes the dominant factor influencing the hydraulic radius as defined by equation (9). For a given type of fabric structure, such as MWAK DOS in this case, higher the fibre volume fraction, smaller is the hydraulic radius and hence greater would be the capillary pressure.

The length of fluid flow in capillary defined in Darcy's equation (1), L (cm), at a given time t (s) is provided by the Washburn equation (10) (Chatterjee and Gupta, 2002) as follows for horizontal capillary wicking, replacing the capillary radius with the hydraulic radius of the fibre bed.

$$L = \sqrt{\frac{m\gamma \cos\theta}{\eta} t} \tag{10}$$

Table 3 provides the calculated values of the hydraulic radius of the fibre bed m (μm), flow length in the capillary L (cm), pressure difference ΔP (dyne/cm^2), permittivity constant K (min) and permeability k (g/cm^2). These values for the given DOS preforms are calculated using the equations (1) and (7)–(10) for a flow of 1 minute time considering the viscosity of water η (0.89 cP).

Analysing the permeability of preform, the low-aerial-density biaxial structure has least in-plane permeability. Triaxial and quadraxial preforms although have comparable fabric aerial density and it can be noticed that the quadraxial structure has high permeability, which could be ascribed to better fibre orientation and higher capillary radius, as evident from low fibre volume fraction value, thus increasing the capillary flow length as explained by the equation (9). It can also be noted that the fibre volume fraction is influencing the fluid flow rate and thus preform permeability as evident from the equations (7)–(9), but the experimental data is inadequate to arrive at this conclusion. The higher wickability of triaxial preforms compared to the biaxial structures could be due to the better fibre orientation and presence of dense capillaries along fibre-oriented directions, but lesser capillary radius would have limited the wickability. Higher fibre volume fractions have shown decreased fluid flow in the triaxial fabric while the highest flow rate in quadraxial preforms has low fibre volume fraction but is most isotropic with respect to fibre orientation which has enhanced the permeability. The Kozeny–Carman relation, for permeability of the porous media with a fibrous architecture is given by equation (11) (Grujicic *et al.*, 2004):

$$k = \frac{d_f^2(1 - V_f)^3}{K_C V_f^2} \tag{11}$$

where d_f, the fibre diameter, V_f, the fibre volume fraction, while K_C is a fibrous-medium architecture-dependent constant known as the Kozeny constant. This Kozeny constant includes a shape factor for the flow channel and a tortuosity factor, the latter usually defined as the ratio of flow channel length to the length of the porous medium. Carmen suggested that empirically K_C is equal to 5 in accordance with the experimental data (Chatterjee and Gupta, 2002). This relation would be of immense aid in comprehending the permeability properties with the compressibility of preforms. The application of these studies would be used to optimize and simulate the RTM process for composite preparation in the future studies.

CONCLUSIONS

The compression behaviour of multiaxial warp-knit preforms shows a particular trend, with total compression amounting to approximately one-third of the preform thickness. Fibre volume fraction of the preform influences the compression behaviour; higher the fibre volume fraction lower is the compressibility of textile preforms. An empirical expression relating fibre volume fraction to preform thickness has been presented.

The fluid flow in-plane permeability studies on directionally oriented warp-knit glass preforms have clearly shown that fibre orientation, preform porosity and presence of capillaries due to fibre orientation in different directions influence preform permeability. Fibre volume fraction of the preform also plays an important role in the permeability as explained by the relations between capillary radius and capillary pressure, but further research is essential to validate this issue. Preform permeability would decrease with increase in compression, and attempts are being made to understand the relations for further application in optimizing and simulating RTM composite preparation.

ACKNOWLEDGMENTS

This work is being conducted within the Asia-Link Programme, project no RP1736, IN/ASIA-LINK/002 (82158). The authors thank the European Commission for awarding a research grant under the EU Asia-Link Project to the Indian Institute of Technology—Delhi (India) and the University of Minho (Portugal). Authors are also thankful to Changzhou Hongfa Composites Engineering Company Limited, China, for providing the samples for the present study.

REFERENCES

Anand, S. C., 1996. Warp knitted structures in composites. In: *7th European Conference on Composite Materials*, London, Vol. 2, pp. 407–413.

ASTM International, 2003. Standard test method for surface wettability and absorbency of sheeted materials using an automated Contact Angle Tester, *ASTM Standard D 5725-2003*, ASTM International, USA.

Cai, Z. and Gutowski, T. G., 1992. The 3-D deformation behavior of a lubricated fiber bundle, *J. Compos. Mater.*, 26, 1207–1237.

Chatterjee, P. K. and Gupta, B. S., 2002. Porous structure and liquid flow models. In: Chatterjee, P. K. and Gupta, B. S. (eds.), *Absorbent Technology, Textile Science and Technology Series*, Elsevier Science, Amsterdam, pp. 1–57.

Chen, B., Cheng, A. H. D. and Chou, T. W., 2001. A nonlinear compaction model for fibrous preforms, *Compos. Pt A*, 32, 701–707.

Chen, B. and Chou, T. W., 1999. Compaction of woven-fabric preforms in liquid composite molding processes: single-layer deformation, *Compos. Sci. Technol.*, 59, 1519–1526.

Chou, T. W., 1992. *Microstructural Design of Fibre Composites*, Cambridge University Press, New York.

Du, G.-W. and Ko, F., 1996. Analysis of multiaxial warp-knit preforms for composite reinforcement, *Comp. Sci. Technol.*, 56(3), 253–260.

Grujicic, M., Chittajallu, K. M. and Walsh, S., 2004. Effect of shear, compaction and nesting on permeability of the orthogonal plain-weave fabric preforms, *Mater. Chem. Phys.*, 86, 358–369.

Gutowski, T. G., 1985. A resin flow/fiber deformation model for composites, *SAMPE Quart.*, 16(4), 58–64.

Gutowski, T. G. and Dillon, G., 1992. The elastic deformation of lubricated carbon fiber bundles: comparison of theory and experiments, *J. Compos. Mater.*, 26, 2331–2347.

Gutowski, T. G. and Dillon, G., 1997. The elastic deformation of fibre bundles. In: Gutowski, T. G. (ed.), *Advanced Composites Manufacturing*, Wiley, New York, pp. 115–156.

Han, K., Lee, W. and Rice, B., 2000. Measurements of the permeability of fibre preforms and applications, *Compos. Sci. Technol.*, 60, 2435–2441.

Hu, J. and Newton, A., 1997. Low-load lateral-compression behaviour of woven fabrics, *J. Text. Inst.*, 88(1), 242–254.

Hoffman, R. M. and Beste, L. F., 1951. Some relation of fibre properties to fabric hand, *Text. Res. J.*, 21, 66–77.

Kamiya, R., Cheeseman, B. A., Popper, P. and Chou, T. W., 2000. Some recent advances in fabrication and design of three-dimensional textile preforms: A review, *Compos. Sci. Technol.*, 60(1), 33–47.

Lai, C. L. and Young, W. B., 1997. Model resin permeation of fibre reinforcements after shear deformation, *Polym. Compos.*, 18(5), 642–648.

Luo, Y., Verpoest, I., Hoes, K., Vanheule, M., Sol, H. and Cardon, A., 2001. Permeability measurement of textile reinforcements with several test fluids, *Compos. Pt A*, 32, 1497–1504.

Matsudaira, M. and Qin, H., 1995. Features and mechanical properties of a fabric's compressional property, *J. Text. Inst.*, 86, 476–486.

NIST, December. 1990. *Proceedings of the Second Industry Workshop on Polymer Composite Processing*, Gaithersburg, MD.

PADAKI, N. V., ALAGIRUSAMY, R. and SUGUN, B. S., 2006. Knitted preforms for composite applications, *J. Ind. Text.*, 35, 295–321.

PATNAIK, A., RENGASAMY, R. S., KOTHARI, V. K. and GHOSH, A., 2006. Wetting and wicking in fibrous materials, *Text. Progr.*, 38(1).

PEARCE, N. and SUMMERSCALES, J., 1995. The compressibility of a reinforcement fabric, *Compos. Manuf.*, 6, 15–21.

PILLAI, K. M., TUCKER, C. L. and PHELAN, F. R., 2001. Numerical simulation of injection/compression liquid composite molding, Part 2: preform compression, *Compos. Pt A*, 32, 207–220.

RANGANATHAN, S., EASTERLING, R. G., ADVANI, S. G. and PHELAN F. R., Jr., 1998. Effect of microstructure variations on the permeability of preform materials, *Polym. Polym. Compos.*, 6(2), 63–73.

RAZ, S., 2000. *The Karl Mayer Guide to Technical Textiles*, Karl Mayer Textilmaschinenfabrik, Germany.

SAUNDERS, R. A., LEKAKOU, C. and BADER, M. G., 1998. Compression and microstructure of fibre plain woven cloths in the processing of composites, *Compos. Pt A*, 29, 443–454.

SAUNDERS, R. A., LEKAKOU, C. and BADER, M. G., 1999. Compression in the processing in the polymer composites, Part I: A mechanical and microstructural study for different glass fabrics and resins, *Compos. Sci. Technol.*, 59, 983–993.

TOLL, S. and MANSON, J. A. E., 1994. An analysis of the compressibility of fibre assemblies In: *6th International Conference on Fibre Reinforced Composites*, Institute of Materials, Newcastle,UK, pp. 25/1–25/10.

VAN WYK, C. M., 1946. Note on the compressibility of wool, *J. Text. Inst.*, 37, T285–T292.

